Title	Effectiveness of Open Boundary Schemes for Long Waves
Author(s)	Hamanaka, Ken-ichiro; Furuya, Atsumi
Citation	Memoirs of the Faculty of Engineering, Hokkaido University, 18(1), 17-27
Issue Date	1990
Doc URL	http://hdl.handle.net/2115/38038
Туре	bulletin (article)
File Information	18(1)_17-28.pdf



Effectiveness of Open Boundary Schemes for Long Waves

Ken-ichiro HAMANAKA Atsumi FURUYA (Received October 15, 1990)

Abstract

The effectiveness of a new numerical scheme of open boundary proposed by Hino (1989), is investigated using of a long wave solution. In the case of one-dimensional propagation in which the waves propagate normal to the open boundary, this scheme predicts almost exact values of the waves transmitting through the boundary. But in the case of two-dimensional propagation, in which the waves propagate obliquely to the open boundary, the estimation by this scheme include significant errors dependent on the phase of waves at the boundary and the incident angle to it. These errors create a artificial reflection. Under an assumption of a steady wave field after the calculation of sufficient number of time steps, the reflection coefficient can be obtained analytically and its correctness can be confirmed in a numerical manner.

1. Introduction

In numerical simulation of propagation of long waves in coastal region, such as tsunami, storm surges and tidal flow etc., it is at times necessary to place an artificial boundary in the ocean, through which the waves are required to propagate freely. This type of artificial boundary is referred to as an open boundary in this paper.

There are many numerical schemes prescribing this open boundary. Which may be categorized into three types; (1) the superposition method with Dirichlet type and Neumann type boundary conditions, (2) the absorption method with the Sommerfeld radiation condition, and (3) the viscous damping (or sponge) method. But each method has its own problems such as (1) complexity of the scheme and its calculation, especially when there are open boundaries that are not limited to one, (2) lack of data regarding wave number vector, and (3) artificial reflection from the sponge layer. The reader should refer a review by Hino (1988), for example.

Recently a numerical scheme of open boundary were proposed by Hino and Nakaza (1988, 1989). This method may be categorized in type (1) mentioned above, and appeas very simple in the physical sense and in the numerical scheme itself. He also emphasized that in his method one is not required to consider the incident angle of waves to the open boundary even in the case of two-dimensional propagation. But there still remains a slight uncertainty.

The purpose of this paper is to check the effectiveness of Hino's scheme by use of a long wave solution. In this paper, only staggered (spatially) and leap-frog (temporally) system is investigated. In onedimensional propagation, his scheme can be

confirmed to satisfy the requirement of open boundary proficiently. In two-dimensional propagation, his scheme has a dual variations. But it is found that each variation includes significant errors depending on the phase of waves at the boundary and incident angle there of. As mentioned in the abstract, these errors create an artificial reflection from the open boundary and will contaminate the computational region.

To investigate this artificial reflection in detail, reflection coefficient is analytically derived under an assumption of a steady wave field. This reflection coefficient can be confirmed to be correct in a numerical manner.

2. The principle of Hino's scheme of open boundary

The principle of Hino's method can be briefly explained as follows. Assuming that the water elevation and the mass flux have been calculated as a freely transmitted wave at the open boundary till the time step n. To estimate the water elevation at the next time step n+1, a temporary rigid wall is instantly placed on that boundary. If the water elevations are calculated in this situation, its value will be composed of the incident wave and the reflected one and will be two fold in value of the elevation of incident wave. Therefore the water elevation at the next time step should be estimated to be half the value calculated under that virtual condition.

3. Error on the open boundary in one time step

3. 1 Finite difference scheme and long wave solution

The finite difference representation of the mass conservation is described in a staggered and leap-frog system under the long wave or the shallow water approximation as follows;

$$\frac{\eta_{i,j}^{n+1} - \eta_{i,j}^{n-1}}{\Delta t} = \frac{M_{i-1,j}^{n} - M_{i+1,j}^{n} + N_{i,j-1}^{n} - N_{i,j+1}^{n}}{\Delta s}$$
(1)

where M and N denote the mass flux between one grid size Δs in x and y direction, respectively. η denotes the water surface elevation, i and j is the spatial grid number in x and y direction. n is the time step number.

The water elevation and the mass flux of a long wave may be represented as

$$\eta = \sin(1x + my - \omega t)
M = C \sin \delta \sin(1x + my - \omega t), N = C \sin \delta \sin(1x + my - \omega t)$$
(2)

where C is the wave velocity. δ is the incident angle so that $\cos \delta = 1/k$ and $\sin \delta = m/k$ with k, the wave number.

3. 2 One dimensional case

We assume that the waves propagate in x direction (δ =0, N=0) and the open boundary is located at x=(i+1) Δ s. Applying Hino's principle into this case with the temporary rigid wall ($M_{l+1,l}^n$ =0) the water elevation at t=(n+1) Δ t is

$$\tilde{\eta}_{i,j}^{n+1} = \frac{1}{2} \left(\frac{\Delta t}{\Delta s} M_{i-1,j}^n + \eta_{i,j}^{n-1} \right)$$
 (3)

Here after, a valuable with the sign tilde denotes the one calculated from a numerical scheme such as Eq.(3). Substituting Eq.(2) into the right hand side of Eq.(3)

$$\tilde{\eta}_{i,j}^{n+1} = \frac{1}{2} \left[\frac{\Delta t}{\Delta s} C \sin\{k(i-f)\Delta s - \omega n \Delta t\} + \sin\{ki\Delta s - \omega(n-1)\Delta t\} \right]$$

$$= \sin(ki\Delta s - \omega n \Delta t)$$

$$= \eta_{i,j}^{n}$$
(4)

with $\Delta s/\Delta t = C = \omega/k$

Therefore Eq.(4) states that the scheme (3) does not predict the water elevation at the time step n+1 but at the time step n. But if the time interval Δt is chosen to be sufficiently small, this error on the water elevation at the time step n+1 may be negligible.

3. 3 Two dimensional case

As mentioned in the introduction, Hino's scheme may heve dual variations in two dimensional case. They are classified into two types.

In the first type, he assumed that the water elevation could be decomposed into x and y components. Then his principle is applied only to x components when the open boundary is located parallel to the y axis. But there may be further slight variations regarding the treatment of water elevation, because of uncertainty of his assumption of decomposition.

Scheme I -1: $\eta_{i,j}^{n-1}$ contributes to y component

$$\tilde{\eta}_{i,j}^{n-1} \text{ contributes to y component}
\tilde{\eta}_{x} = \frac{1}{2} \frac{\Delta t}{\Delta s} M_{i-1}^{n} = \frac{1}{2} \left(\cos \delta \sin \theta - \omega \Delta t \cos^{2} \delta \cos \theta \right)
\tilde{\eta}_{y} = \frac{\Delta t}{\Delta s} \left(N_{i,j-1}^{n} - N_{i,j+1}^{n} \right) + \eta_{i,j}^{n-1}
= -2\omega \Delta t \sin^{2} \delta \cos \theta + \sin \theta + \omega \Delta t \cos \theta$$
(5)

Scheme I -2: $\eta_{i,i}^{n-1}$ contributes to x component

$$\tilde{\eta}_{x} = \frac{1}{2} \left(\frac{\Delta t}{\Delta s} M_{i-1}^{n} + \eta_{i,j}^{n-1} \right)
= \frac{1}{2} (\cos \delta \sin \theta - \omega \Delta t \cos^{2} \delta \cos \theta + \sin \theta + \omega \Delta t \cos \theta)
\tilde{\eta}_{y} = \frac{\Delta t}{\Delta s} (N_{i,j-1}^{n} - N_{i,j+1}^{n}) = -2\omega \Delta t \sin^{2} \delta \cos \theta$$
(6)

where $\theta = il\Delta s + jm\Delta s - n\omega\Delta t$ with $l\Delta s \ll 1$, $m\Delta s \ll 1$ and $\omega\Delta t \ll 1$. And then, in both cases

$$\tilde{\eta} = \tilde{\eta}_{1,j}^{n+1} = \tilde{\eta}_{x} + \tilde{\eta}_{y} \tag{7}$$

On the other hand, the water elevation of long wave solution Eq. (2) is;

$$\eta = \eta_{\rm h,l}^{n+1} = \sin \theta - \omega \Delta t \cos \theta \tag{8}$$

Fig. 1 shows the error $\text{Er} = \tilde{\eta} - \eta$ against the phase of waves at the open boundary with the incident angle as a parameter. The curve at the left end of the top line of each a) and b) is the water elevation on the boundary. These figures state that both schemes I -1 and I-2 have same significant errors. But scheme I-1 is relatively effective when the waves propagate parallel to the boundary and scheme I-2 is such that when the waves propagate normal to the boundary.

In the second type, the temporary rigid wall is assumed to be located in both directions of x and y on the open boundary to avoid the uncertainty of the decomposition of water elevation.

Scheme II—1

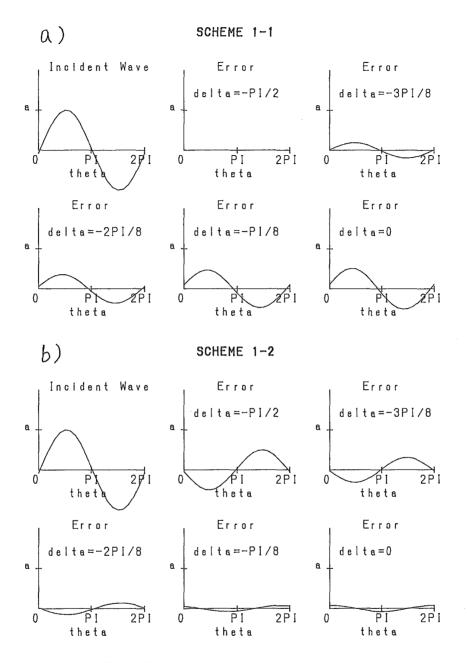


Fig. 1 Errors of a): Scheme I-1 and b): Scheme I-2

$$\tilde{\eta}_{i,j}^{n+1} = \frac{1}{2} \left\{ \frac{\Delta t}{\Delta s} \left(M_{i-1,j}^{n} + N_{i,j-1}^{n} \right) + \eta_{i,j}^{n-1} \right\}$$

$$= D_{1} \sin \theta = D_{1} \eta_{i,j}^{n}$$

$$(9)$$

where $D_1 = \frac{\sqrt{2 \cos \delta - \pi/4 + 1}}{2}$

In this case, the estimation on water elevation at the time step n+1 becomes the coefficient D_1 times the water elevation at the time step n. Therefore if the difference

between η^{n+1} and η^n is sufficiently small, D_1 mainly contributes to the effectiveness of this scheme. a) of Fig. 2 shows D_1 against the incident angle. It is found that this scheme is relatively effective when the waves come from the right hand side to the boundary.

To avoid this asymmetry of scheme II—1, it can be easily imagined to take an average of the estimations of the type of scheme II—1 with the temporary rigid walls placed on the right hand side and the left hand side.

Scheme II-2

$$\tilde{\eta}_{i,j}^{n+1} = \frac{1}{2} \left[\frac{1}{2} \left\{ \frac{\Delta t}{\Delta s} \left(M_{i-1,j}^{n} + N_{i,j+1}^{n} \right) + \eta_{i,j}^{n-1} \right\} + \frac{1}{2} \left\{ \frac{\Delta t}{\Delta s} \left(M_{i-1,j}^{n} - N_{i,j-1}^{n} \right) + \eta_{i,j}^{n-1} \right\} \right] \\
= D_{sin} \theta \tag{10}$$

where $D_2 = (\cos \delta + 1)/2$

b) of Fig. 2 shows D₂ against the incident angle. In this case, the effectiveness of this

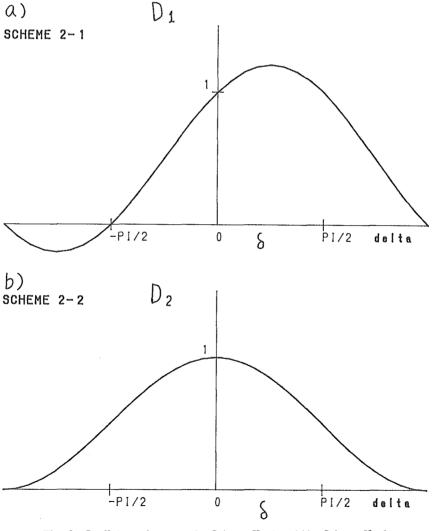


Fig. 2 Coefficient of errors, a): Scheme II-1 and b): Scheme II-2

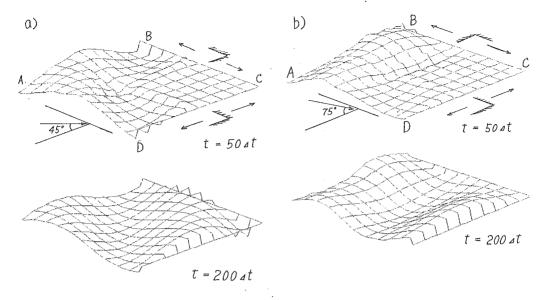


Fig. 3 Wave propagation through the open boundary of Scheme II—1

- a) advantageous configuration
- b) disadvantageous configuration

scheme has a symmetry to the open boundary as expected.

To check the analysis mentioned above, some calculation were performed. Fig. 3 is one example using scheme II—1 as the open boundary. The incident wave comes into the computational region from the left hand side of the figure and the sides BC and DC are the open boundaries. In a) of the figure, the temporary rigid walls were arranged in an advantageous manner on both sides BC and DC. But in b) this wall were arranged in the disadvantageous manner on the BC side. As a result, undesirable reflection took place from the BC side and distorted the incident waves.

4. Generalization of Hino's scheme and artificial reflection coefficient

Four types of variations of Hino's scheme were investigated in the previous section. In these variations, the water elevation on next time step were estimated from the previous water elevation and three neighboring mass fluxes. In this sense, we can generalize the Hino's scheme;

$$\tilde{\eta}_{i,j}^{n+1} = \frac{\Delta t}{\sqrt{s}} \left(\alpha_1 M_{i-1,j}^n + \alpha_2 N_{i,j-1}^n + \alpha_3 N_{i,j+1}^n \right) + \alpha_4 \eta_{i,j}^{n-1}$$
(11)

The errors of this scheme from the long wave solution can be calculated along the same way of the previous section. These errors are produced in one time step calculation and will be carried to the next time step on the open boundary through the numerical scheme Eq.(11) and inside the computational region through the general finite difference scheme. Then they will be added to the new errors on the boundary at this new time step, and so on. As a result, these errors create artificial reflected waves. To analyze how these reflected waves develop as the calculation proceeded, may be quite difficult, because of the unsteadiness in the beginning of the calculation. But when the calculation has been proceeded a sufficient number of time steps, it could be

assumed that the incident and reflected waves have formed a steady wave field. In this case, the incident and reflected waves should exactly satisfy the Eq. (11), together. Then this condition will determine the reflection coefficient.

The open boundary is assumed to be located at the same place as that of the previous section at $x=(i+1)\Delta s$. The incident and reflected waves are represented in the same way of Eq.(2) with subscripts I and R, denoting incident and reflected waves, respectively.

$${}_{1}\eta = \sin(1x + my - \omega t)$$

$${}_{1}M = \frac{1}{k}C\sin(1x + my - \omega t), \ {}_{1}N = \frac{m}{k}C\sin(1x + my - \omega t)$$
(12)

$${}_{R}\eta = R \sin(-1x + my - \omega t + \sigma)$$

$${}_{R}M = -R \frac{1}{k} C \sin(-1x + my - \omega t + \sigma), \ {}_{R}N = R \frac{m}{k} C \sin(-1x + my - \omega t + \sigma)$$

$$(13)$$

$$\eta = {}_{1}\eta + {}_{R}\eta, M = {}_{1}M + {}_{R}M, N = {}_{1}N + {}_{R}N$$
(14)

Substituting Eq.(14) into Eq.(11) with Eq.(12) and (13), we obtain the water elevation at next time step n+1.

$$\tilde{\eta}_{i,j}^{n+1} = {}_{1}\tilde{\eta}_{i,j}^{n+1} + {}_{R}\tilde{\eta}_{i,j}^{n+1}
= P_{1}\sin\theta + P_{2}\cos\theta + R P_{3}\sin\theta' + R P_{2}\cos\theta'$$
(15)

where $P_1 = \{\beta \left(\alpha_1 \frac{1}{k} + \alpha_2 \frac{m}{k} + \alpha_3 \frac{m}{k}\right) + \alpha_4\}$

$$P_2 = \gamma \{-\alpha_1 \left(\frac{1}{k}\right)^2 - \alpha_2 \left(\frac{m}{k}\right)^2 + \alpha_3 \left(\frac{m}{k}\right)^2 + \alpha_4 \}$$

$$P_3 = \{\beta \left(-\alpha_1 \frac{1}{k} + \alpha_2 \frac{m}{k} + \alpha_3 \frac{m}{k}\right) + \alpha_4\}$$

with $\theta' = \theta + \sigma$, $\beta/C = \Delta t/\Delta s$, $\gamma = \omega \Delta t$

On the other hand, the water elevation of the long wave solution at the same time step is given from Eq.(12) and (13).

$$\eta_{i,j}^{n+1} = \sin \theta - \omega \Delta t \cos \theta + R \sin \theta' + R \omega \Delta t \cos \theta' \tag{16}$$

That Eq.(15) is equal to Eq.(16) must be satisfied for all values of y and t. This lead us to the evaluation of the reflection coefficient.

$$R = \sqrt{(P_1 - 1)^2 + (P_2 + \gamma)^2} / \sqrt{(P_3 - 1)^2 + (P_2 + \gamma)^2}$$
(17)

The solid curves of Fig. 4 and 5 show the reflection coefficiet against the incident angle, Eq.(17), of the scheme II—1 with β and γ as parameters. Fig. 6 shows that of the scheme II—2. The reflection coefficient of the scheme II—1 is asymmetric concerned with the incident angle as expected from the previous analysis and appears to have reasonable values except that at $\delta = \pi/2$ where the reflection coefficient takes large value. In the case of $\delta = \pi/2$, the wave propagates parallel to and advantageous direction to the open boundary. The analysis of the previous section states that the error produced within one time step is very small with the small value of Δt .

To confirm the correctness of the result of the reflection coefficient, two or more numerical simulations were performed. The incident waves come into the computational region ABCD (see Fig. 7 and 8) through the boundary AD with a suitable incident angle. The side AB is a open boundary to be checked. The error produced within one time step can be given from Eq.(15) and Eq.(16);

REFLECTION COEFFICIENT R alpha 1 - alpha 4 = .5 .5 .5 0 .5 beta = .626 gamma = .251 o

Fig. 4 Reflection coefficient Scheme II—1 $\beta = .625$ $\gamma = .251$

0

P1/2

PI/2

-PI/2

-PI/2

REFLECTION COEFFICIENT R alpha 1 - alpha 4 = .5 .5 .5 0 .5 beta = .626 gamma = .126

Fig. 5 Reflection coefficient Scheme II—1 $\beta = .625$ $\gamma = .125$

Fig. 6 Reflection coefficient Scheme II—2 $\beta = .625$ $\gamma = .125$

0

$$\eta_{\rm E} = {}_{1}\eta_{\rm i,j}^{\rm n+1} - {}_{1}\tilde{\eta}_{\rm i,j}^{\rm n+1} = (1 - {\rm P}_{1})\sin\theta - (\gamma + {\rm P}_{2})\cos\theta \tag{18}$$

Therefore only this error, Eq.(18), was added to each time step along the side AB, instead of giving the original incident wave itself on side AD. The scheme II—1 were installed on each boundary and a general finite difference—scheme was used inside the computational region. Then the only artificial reflected waves can be seen in this simulation. After sufficient time steps of computation, the wave field could be confirmed to be almost stationary.

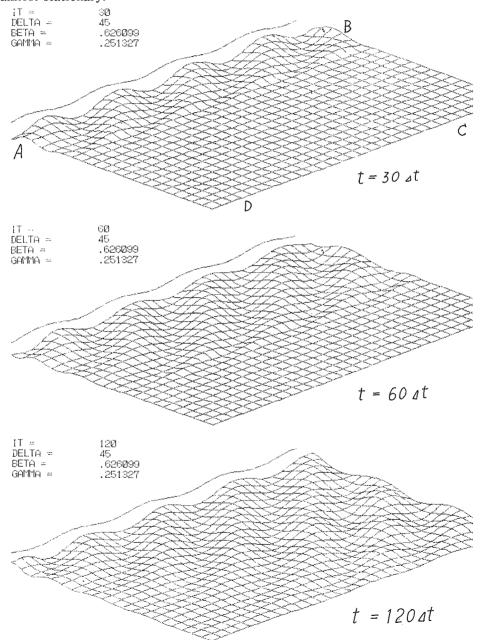


Fig. 7 Development of reflection The incident angle is 45°

Fig. 7 shows the propagation and the development of the artificial reflection when the waves attack the open boundary at the angle $\pi/4$, and Fig. 8 at the angle $\pi/2$ (waves are propagating parallel to the open boundary). Both are up to 120 time steps. The amplitudes of these reflected waves were measured numerically and the reflection coefficients were calculated. The circles in Fig. 4 and 5 are the reflection coefficients calculated in this simulation.

They have good agreements with the reflection coefficients obtained analytically.

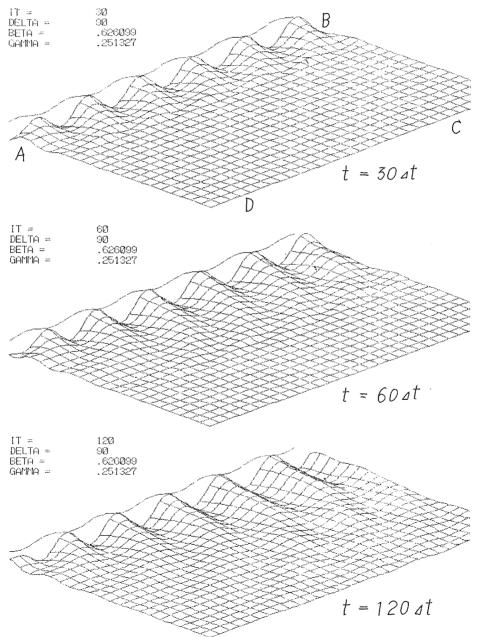


Fig. 8 Development of reflection The incident angle is 90°

From this investigation, it is found that when the waves propagate almost parallel to an open boundary even in the advantageous direction, the errors produced on the open boundary tend not to diverge inside the computational region but to accumulate near the boundary. Therefore the reflection coefficient becomes large even though the error within one time step is small.

5. Conclusion

- (1) The errors of Hino's open boundary scheme from the long wave solution within one time step were evaluated. The errors were found to depend on the incident angle of waves to the open boundary.
- (2) The reflection coefficient of reflected waves created by the errors on the generalized open boundary scheme were analyzed under the assumption of a steady wave field. Applying this analysis to Hino's scheme, it was found that when the waves propagated parallel to the open boundary, the errors tended to accumulate on the open boundary and create large reflected waves.
- (3) When a specified sea or a bay is chosen to be investigated, a suitable scheme of open bouundary must be chosen under the consideration on the direction of the waves and position of the open boundary.
- (4) Using the representation of the reflection coefficient, Eq.(17), the most suitable coefficient of the general expression of open boundary scheme Eq.(11) may be possible to be determined by means of the least square method.

References

Hino, M. (1988) A short review on numerical methods of open boundary, Tech. Report No. 39, Dept. of Civil Eng., Tokyo Inst. of Tech. (in Japanese)

Hino, M. and Nakaza, E. (1988) Test of a new numerical scheme of open boundary for the two dimensional cases, Proc. 35th Japanese Conf. on Coastal Eng., pp 262-266

Hino, M. and Nakaza, E. (1989) Test of a new numerical scheme on a "nonreflection and free-transmission" open-sea boundary for longwaves, Fluid Dynamics Research, Vol. 4, pp 305-316